

Rapid and Accurate Pressure Sensing Device for Direct Measurement of Intraocular Pressure

Tilvawala Gopesh¹, Andrew Camp², Michael Unanian¹, James Friend¹,
and Robert N. Weinreb²

¹ Medically Advanced Devices Laboratory, Center for Medical Devices and Instrumentation, Department of Mechanical and Aerospace Engineering, University of California, San Diego, La Jolla, CA, USA

² Hamilton Glaucoma Center, Shiley Eye Institute and the Viterbi Family Department of Ophthalmology, University of California, San Diego, La Jolla, CA, USA

Correspondence: Robert N. Weinreb, Hamilton Glaucoma Center, Shiley Eye Institute and the Viterbi Family Department of Ophthalmology, University of California, San Diego, 9415 Campus Point Dr, La Jolla, CA 92093, USA. e-mail: rweinreb@ucsd.edu;

James Friend, Department of Surgery, University of California, San Diego, 9300 Campus Point Drive, La Jolla, CA 92037-7400, USA. e-mail: jfriend@ucsd.edu

Received: June 5, 2019

Accepted: December 6, 2019

Published: February 25, 2020

Keywords: glaucoma; intraocular pressure; manometry

Citation: Gopesh T, Camp A, Unanian M, Friend J, Weinreb RN. Rapid and accurate pressure sensing device for direct measurement of intraocular pressure. *Trans Vis Sci Tech.* 2020;9(3):28, <https://doi.org/10.1167/tvst.9.3.28>

Purpose: Intraocular pressure (IOP) is the primary modifiable risk factor for glaucoma. Current devices measure IOP via the dynamic response of the healthy cornea and do not provide the accurate IOP measurements for patients with altered corneal biomechanics. We seek to develop and test an accurate needle-based IOP measurement device that is not cornea dependent.

Methods: Our device combines a high-resolution pressure microsensors with 30- and 33-gauge Luer lock needles to provide IOP measurements via a microcontroller and USB interface to a computer. The device was calibrated in a membrane chamber and then tested and validated in the anterior chamber and post-vitreotomy vitreous chamber of rabbit eyes. The results were compared to Tonopen readings across a pressure range of 0 to 100 mm Hg, imposed in increments of 10 mm Hg.

Results: Both the needle based sensor device and the Tonopen demonstrated a linear relationship with changes in imposed pressure. The Tonopen was found to consistently underestimate the IOP both in the anterior and vitreous chambers. The Tonopen exhibited a significantly greater error than our needle-based sensor device. With increased pressure (>30 mm Hg), the error of the Tonopen increased, whereas the error of our device did not. The 30-gauge needle produces an insignificant improvement in accuracy over the 33-gauge needle.

Conclusions: A needle-based sensor device enables accurate IOP measurements over a broad range of induced IOP.

Translational Relevance: Direct measurement of IOP in the anterior chamber circumvents the influence of corneal parameters on IOP measurement.

Introduction

Intraocular pressure (IOP) is the primary modifiable risk factor in the development and progression of glaucoma. Reliable measurements of IOP are crucial in the management of this sight-threatening disease. The gold standard for IOP measurement for more than 50 years has been Goldmann applanation tonometry (GAT).¹ GAT is a noninvasive measurement technique

that infers IOP from the force required to flatten a portion of the cornea.

However, accurate GAT assessment of IOP is dependent on an ideal eye and can be affected by many factors including corneal thickness, corneal curvature, and irregular corneal biomechanical properties.² Furthermore, GAT is not possible in patients with a Boston keratoprosthesis (KPro) because of the inelasticity of the implant.

New technologies have attempted to address the shortcomings of GAT. The accuracy of dynamic contour tonometry is less affected by corneal thickness than corneal curvature.³ The ocular response analyzer likewise is less influenced by corneal properties and provides measures of corneal biomechanics through corneal hysteresis.⁴ The Diaton tonometer (Ryazan State Instrument-Making Enterprise, Ryazan, Russia) measures IOP through transpalpebral tonometry and can be used to measure IOP in KPro patients, but the device is not very accurate.⁵ Implantable IOP measurement devices circumvent potential artifacts by directly measuring IOP but require a surgical procedure.^{6,7}

Intravitreal injections for the treatment of retinal disorders are performed millions of times per year.⁸ Intravitreal injections have been widely adopted due to their favorable safety profile, with infections associated with fewer than 1 in 6000 injections.⁹ Anterior chamber paracentesis is less common but is also safe and has a low risk of iatrogenic complications.¹⁰ This presents the possibility of directly measuring intraocular pressure in the anterior or vitreous chambers. Advances in micromanometric technology have made this increasingly feasible for the clinician. Previous studies have demonstrated the use of needles inserted directly into the eye to measure pressure, but these devices were not hand-held, used larger-gauge needles, measured the pressure imposed from an upstream reservoir rather than a direct measure of anterior chamber pressure, and are not disposable.^{11–14} In 1 study the results of upstream measurements were confirmed with direct measurements from the anterior chamber, but this required a large 23-gauge needle and was conducted at specific pressures of 20 and 60 mm Hg.¹⁴ Here, we present a novel direct IOP measurement device that provides rapid and accurate measurements and is independent of the cornea. The device is ergonomic and hand-held and has a disposable needle and sensor that can be discarded after use. The device was tested *ex vivo* in rabbits and accurately measured IOP in the anterior chamber and vitreous chamber of vitrectomized eyes.

Methods

Micromanometry System

A high-resolution pressure sensor (2SMPP-03; Omron, Kyoto, Japan), suitable for both pneumatic and hydraulic sensing, was integrated with a custom designed circuit that enables obtaining accurate measurements of the IOP via a USB interface as

shown in [Figure 1](#). The pressure sensor and circuit were assembled in a custom designed, 3-dimensional printed, and palm-sized housing. The assembled device is comprised of an acquisition circuit and disposable unit that includes the pressure sensor and needle. A 30- or 33-gauge needle (PRE-33013; TSK Laboratory, Tochigi, Japan) was primed with sterile balanced salt solution (BSS) and connected to a pressure sensor through a Luer Lock mechanism. Analog signal delivered from the pressure sensor was converted to digital via an Arduino Due (ADU, A000062; Arduino, Ivrea, Italy) board at an acquisition rate of 50 ms (20 Hz). Internal circuitry ensures that pressures outside the measurement range do not create voltages large enough to damage the Arduino Due. This is achieved via a Wheatstone bridge built into the pressure sensor. The voltage is then amplified with a precise gain using an instrumentation amplifier (INA126; Texas Instruments, Dallas, TX) that sets the sensitivity of the pressure measurement. The output is then limited using 2 limiter circuits; 1 for the upper bound and the other for the lower bound of the expected pressure range. The upper and lower bounds are set by the internal ADC of the Arduino Due, but the sensitivity of the measurement can be changed by adjusting the feedback resistor of the instrumentation amplifier. The internal Arduino Due ADC then digitizes the analog signal at a user-defined sampling rate. The digital signal transmitted to a computer through a standard USB interface was used to infer the output reading in millimeters of mercury based on calibration measures described below.

Calibration and Testing

A high-resolution microfluidics pressure control system (microfluidics control, OB1; Elveflow, Paris, France) was used to control the pressure imposed on the pressure sensor to produce a calibration curve. This was obtained in the first instance by connecting the microfluidics control system to the sensor needle through an elastic membrane to better represent an actual eye. This test was conducted to ensure the sensitivity of the micromanometric system was sufficient to capture the changes imposed by the microfluidics control system and subsequently obtain the calibration equation for the sensor. An elastic *ex vivo* model of the eye was constructed to which the microfluidics control system was connected using a 25-gauge needle (25G 1, BD Eclipse; Becton Dickinson, Franklin Lakes, NJ). The elastic model is a closed membrane chamber comprised of a polymer with mechanical properties similar to a cornea.¹⁵ The membrane chamber was filled with BSS and a vacuum

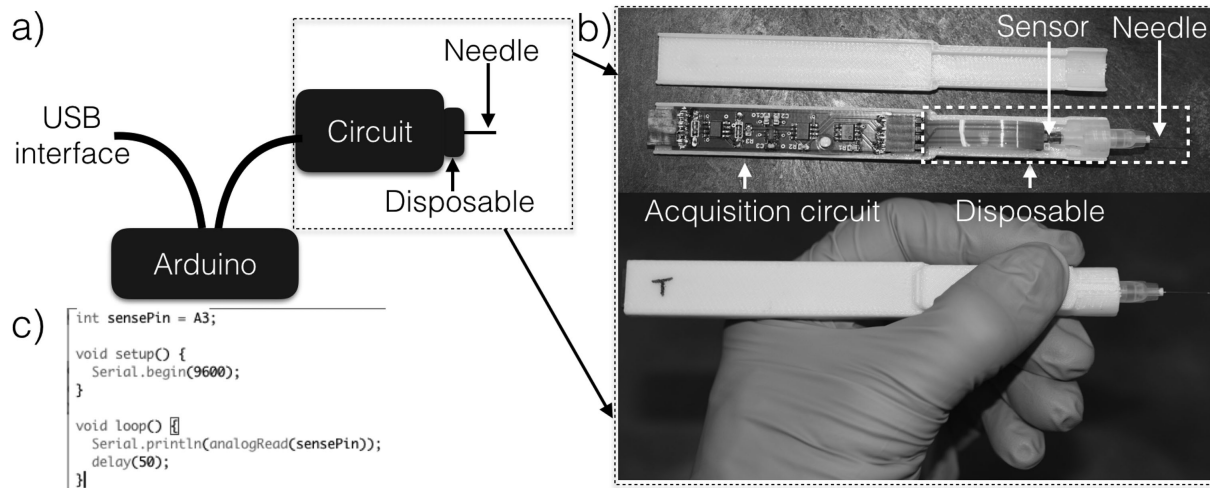


Figure 1. (a) Illustration of the device acquisition set-up. (b) Image of the circuit and disposable part which get assembled in a custom 3-dimensional printed housing. (c) The code for the Arduino used to acquire data.

chamber was used to eliminate dissolved air that could later lead to entrapped air bubbles. The microfluidics control system added or removed BSS in the membrane chamber to increase or decrease the pressure of the system. The needle sensor device was connected to the closed chamber with either of 2 needle sizes (30-g \times 1/2 in and 33-g \times 1/2 in), effectively submerging the sensor in BSS, and the pressure was varied using the microfluidics control system. Sensor readings were recorded while increasing the pressure from 0 to 103.4 mm Hg (2 Psi), and back to 0 with steps of 10.3 mm Hg (0.2 Psi). The readings were used to calibrate the sensor relative to the pressure imposed by the microfluidics control system. Linear regression analysis was used to compute the R^2 values and establish a linear correlation between the sensor readings (S) and the imposed pressure (P_{IN}) such that $S = aP_{IN} + b$, where a and b are correlation coefficients. The sensor needle device was then tested in ex vivo rabbit eyes. Rabbits killed after nonophthalmic studies were obtained through a tissue transfer agreement approved by the University of California San Diego Institutional Animal Care and Use Committee, and all work was performed in adherence to the ARVO Statement for the Use of Animals in Ophthalmic and Vision Research. The microfluidics control system was connected to a 25-gauge needle and inserted into the anterior chamber of the eyes. The sensor needle was then inserted into the anterior chamber and likewise maintained in a fixed position on a stabilizer arm as shown in Figure 2. Although the device can be hand held during measurements,

the stabilizer arm was used because of the number of measurements taken. Two needle sizes, 30-g \times 1/2 in and 33-g \times 1/2 in, were used to obtain sensor readings for the pressure changes in the anterior chamber. After obtaining readings with one needle, the disposable unit comprising of the pressure sensor and needle was replaced with a new unit using a push-fit connection to obtain the next set of readings.

The input pressure in the anterior chamber pressure was varied from 0 to 103.4 mm Hg (2 Psi) in 10 mm Hg (0.2 Psi) increments. The device was evaluated using the calibration equation from the elastic membrane chamber, $P_M = \frac{S-b}{a}$, where P_M is the measured pressure, S is the sensor reading, a and b are the linear correlation coefficients. The IOP was also measured using a Tonopen after the device reading for each increment in pressure.

Measurements were repeated for 5 eyes using both needle sizes (10 eyes total), replacing the disposable unit comprised of the sensor and needle with a new unit using a push-fit connector.

The tests were repeated in the vitreous chamber of vitrectomized rabbit eyes. Similar to the anterior chamber measurements, a 25-g needle attached to the microfluidics control system was inserted into the vitreous chamber and held in a fixed position using a stabilizer arm. The sensor needle was inserted into the vitreous chamber and 2 needle sizes, 30-g \times 1/2 in and 33-g \times 1/2 in, were again used to measure the pressure changes in the vitreous chamber.

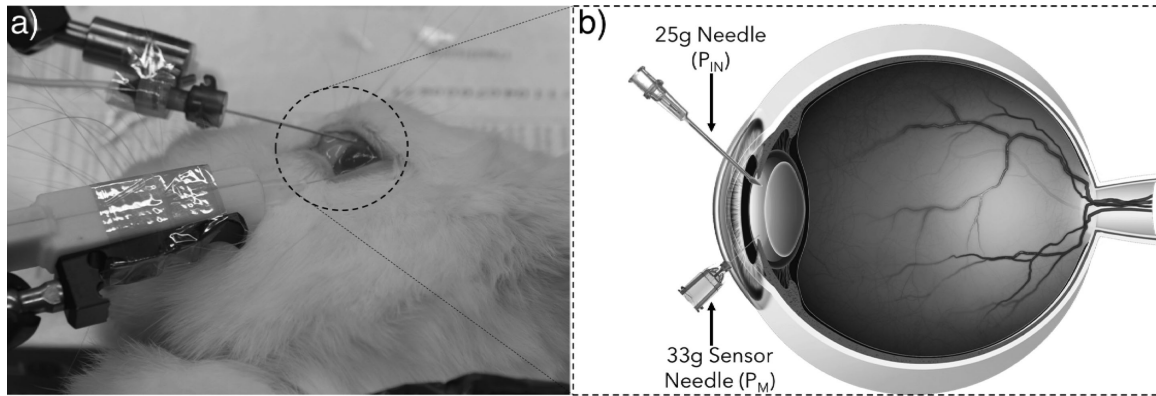


Figure 2. (a) Image of the test setup in rabbit eyes and (b) illustration of supply pressure and sensor needle. The 25-g needle was used to supply pressure from the microfluidics control system and the sensor needle used to measure the pressure change in the anterior chamber.

The pressure imposed by the microfluidics control system was varied from 0 to 103.4 mm Hg (2 Psi) in 10 mm Hg (0.2 Psi) increments and sensor readings taken at each increment. The IOP was also measured using a Tonopen simultaneously with the sensor readings.

Results

Calibration

The sensor of the micromanometry system was tested through a connection to an elastic membrane chamber that exhibits a linear relationship with the pressure imposed by the microfluidics control system for both the needles, 30-g \times 1/2 in and 33-g \times 1/2 in. Scatter plots of the pressure recorded by the sensor needle device against the pressure imposed by the microfluidics control system are shown in Figure 3.

The sensor reading is linearly dependent ($R^2 > 0.99$) over 0 to 103.4 mm Hg, and the change in the reading in replacing a 30-g needle with a 33-g needle is insignificant according to a paired *t*-test ($P < 0.05$). The results indicate the sensitivity of the device is sufficient to capture the changes imposed by the microfluidics control system over a pressure range of 0 to 103.4 mm Hg (2 Psi), with increments of 10.3 mm Hg (0.2 Psi). The calibration equations for the sensor in an elastic membrane chamber measurements are shown in the Table, where the sensor reading, *S*, is expressed as a linear function of the imposed pressure, P_{IN} .

Ex Vivo Rabbit Eyes

The same test was conducted in rabbit eyes, with the sensor acquisition rate at 50 ms (20 Hz) for both the

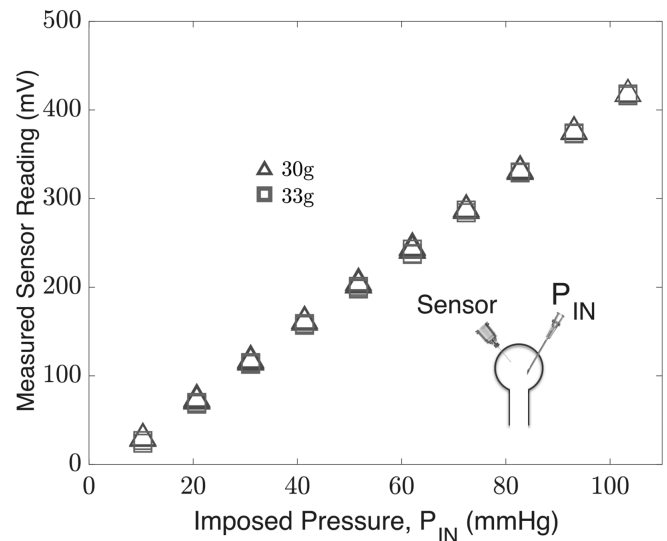


Figure 3. Sensor needle device readings obtained by connection to the microfluidics control system in an elastic membrane chamber using 30-g \times 1/2 in and 33-g \times 1/2-in needles.

Table. Sensor Needle Device Calibration Equations

Equation	Needle	
$S = aP_{IN} + b$	30-g	33-g
a	4.16	4.18
b	-13	-17

needles, 30-g \times 1/2 in and 33-g \times 1/2 in. The calibration equations from the elastic membrane chamber (Table) were used to infer the IOP from the sensor needle device such that: $P_M = \frac{S+13}{4.16}$ (30-g needle) and $P_M = \frac{S+17}{4.18}$ (33-g needle), where P_M is the measured pressure and *S* is the sensor reading. The sensor device

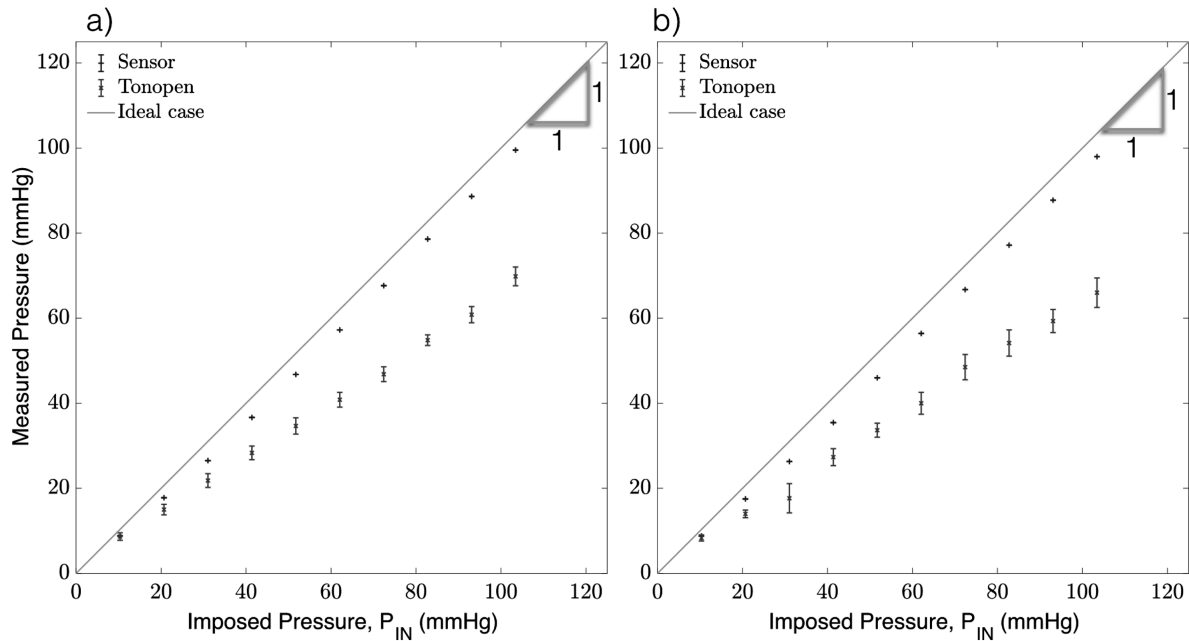


Figure 4. Anterior chamber pressure measurements using the sensor needle device and tonometry for (a) 30-g needle and (b) 33-g needle.

measurements were compared against those obtained by the Tonopen. The results in Figure 4 demonstrate the accuracy of the device with a strong linear correlation between the imposed (P_{IN} , x-axis) and measured (P_M , y-axis) pressure for both the 30-g and 33-g needles. The coefficient of determination (R^2) was excellent for both needle sizes ($R^2 = 1.0$ and 0.99 for the 30- and 33-g needles, respectively), and the Tonopen in both trials ($R^2 = 0.98$ and 0.99). The data was confirmed to be normal via the Shapiro-Wilk test with significance $P < 0.05$ and $n = 10$. Pooled variances for the readings were used to determine the average standard deviation of each measurement device. The average standard deviation of the 30- and 33-g needles (1.32 and 2.7 mm Hg, respectively) were much smaller than that of the Tonopen in either trial (6.12 and 9.02 mm Hg, respectively).

The relative error was evaluated as $\frac{P_{IN} - P_M}{P_{IN}}$, where P_{IN} is the pressure imposed by the microfluidics control system, and P_M is the pressure measured by either the sensor needle device or the Tonopen. The Tonopen underestimates the delivered pressure, particularly at higher pressures, where the relative error for readings obtained by the Tonopen compared to the sensor needle are significantly larger as shown in Figure 5. In contrast, the sensor needle device exhibits higher accuracy at higher pressures.

The tests were repeated in the vitreous chamber of vitrectomized rabbit eyes. Results in Figure 6 show the coefficient of determination was excellent for both

needle sizes ($R^2 = 1$ and 0.998 for 30- and 33-g needles, respectively). By comparison, the Tonopen readings exhibit a slightly lower coefficient of determination ($R^2 = 0.97$ and 0.98 , for tests with the 30- and 33-g needles, respectively).

The Tonopen also underestimates the pressure readings by over 20% on average as shown in Figure 7. The slightly higher error for the 33-g in comparison to the 30-g needle can be attributed to the loss in pressure transmission across the smaller needles' lumen when transmitting pressure from the vitreous chamber to the pressure sensor.

Discussion

Advances in microfabrication have allowed the construction of increasingly sophisticated devices well suited to the small dimensions of the eye. Using the technology described above, a high-resolution pressure sensor was integrated with a 30- and 33-gauge needle to accurately and reliably measure IOP in the anterior and vitreous chambers. Notably, the device provides a direct measure of IOP that is not affected by corneal properties. The device accurately measured IOP in the anterior chamber over a clinically significant range of 10 to 100 mm Hg (Figure 4). In contrast, the Tonopen underestimated the IOP, particularly at higher pressures. This finding is consistent

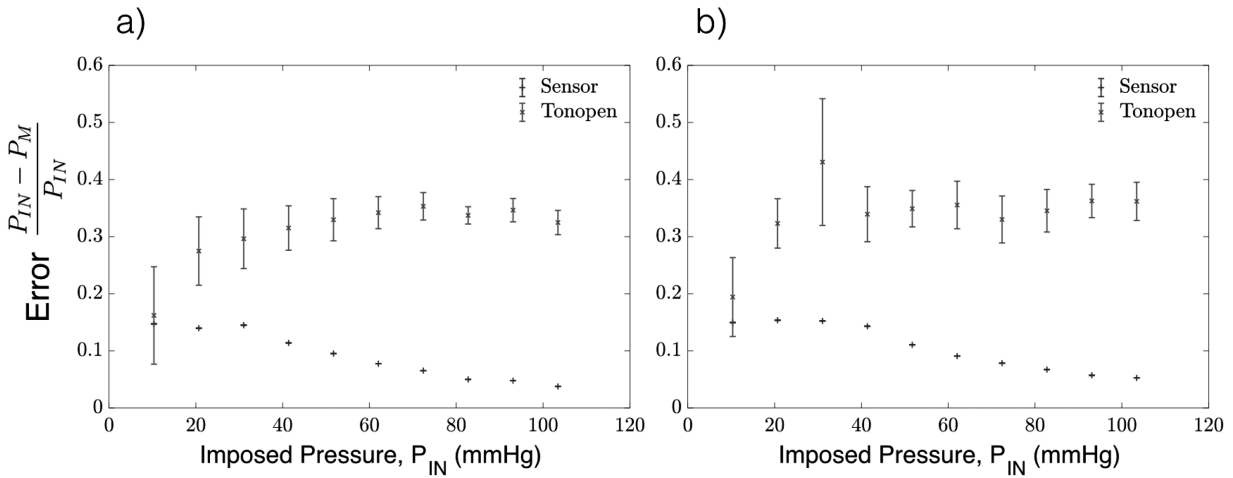


Figure 5. Error in the anterior chamber pressure measurements using the sensor needle device and tonometry for (a) 30-g needle and (b) 33-g needle.

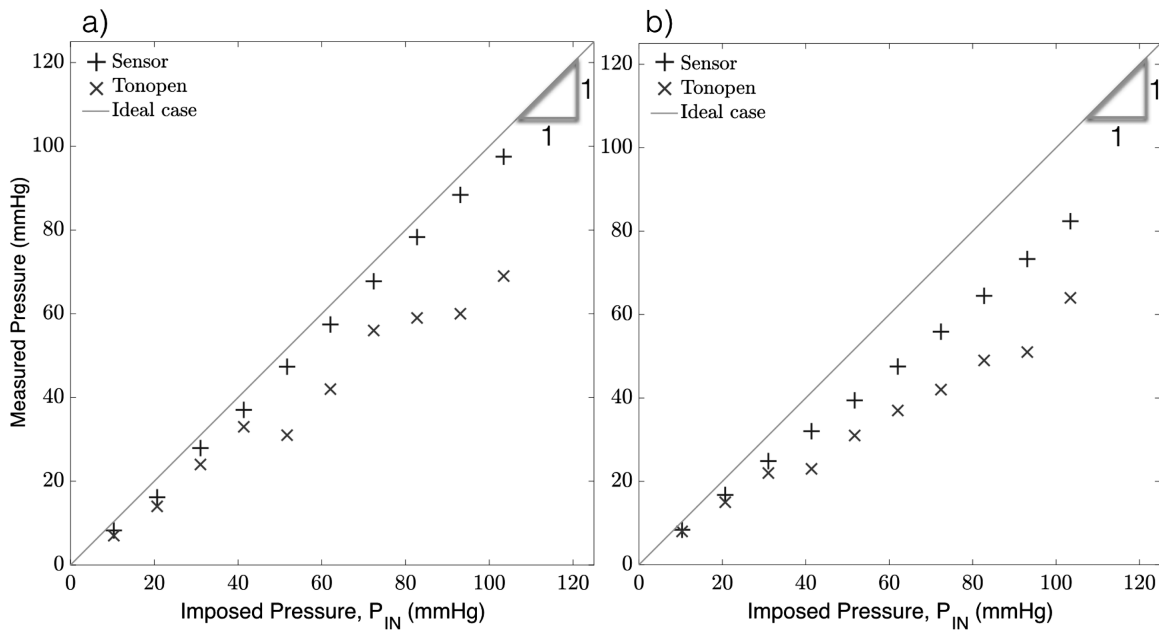


Figure 6. Vitreous chamber pressure measurements obtained using the sensor needle device and tonometry for (a) 30-g needle and (b) 33-g needle.

with prior studies showing the Tonopen underestimates IOP in rabbits.¹⁶ IOP measurements in rabbits can be corrected to account for thinner corneas leading to the underestimation of their IOP.¹⁷ Similar correction factors exist for humans, but their use may not lead to increased accuracy in IOP estimation due to many other factors that may induce artifacts.¹⁸ More complex models that attempt to address additional factors such as the modulus of elasticity are still prone to error.^{19,20} A history of refractive surgery may lead to further inaccuracies in the measurement of IOP

due to thinning of the cornea, changes in the corneal curvature, and alterations in the corneal biomechanical properties.²¹⁻²³ Corneal scars may influence IOP in even more unpredictable ways due to their varying sizes, depths, and effects on the cornea's biomechanical properties.²⁴ All of these potential sources of error are frequently encountered in the clinical setting, yet there are limited means to address them. Our device allows for an accurate measurement of IOP in any of these cases. The patient may not need this measurement repeated at every visit if the results are reassuring

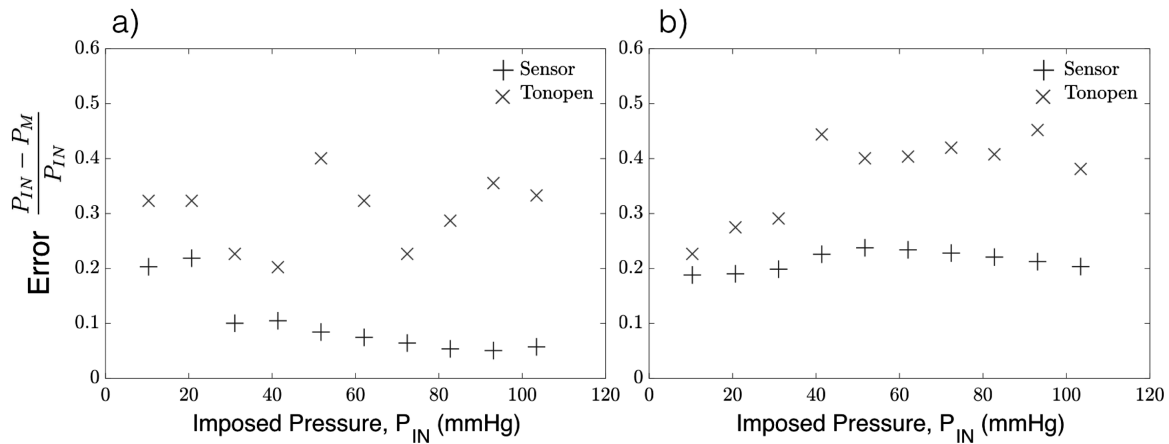


Figure 7. Error in the vitreous chamber pressure measurements using the sensor needle device and tonometry for (a) 30-g needle and (b) 33-g needle. As the imposed pressure (P_{IN}) increases, the error for the readings obtained by tonometry fluctuate or get larger while the sensor needle device stabilizes.

or can be correlated to GAT or another noninvasive measurement technique. However, the opportunity for direct IOP measurement would be a useful addition to a clinician's armamentarium.

The device also accurately measured IOP in the vitreous chamber after vitrectomy (Figure 6). We were unable to measure IOP in the vitreous chamber without vitrectomy because vitreous rapidly clogged the measurement needle, voiding the sensor reading. A similar result was found in prior cannulation studies.²⁵ However, despite this limitation, direct measurement of IOP in the vitreous chamber after vitrectomy is clinically useful. As many as 60% of Kpro patients develop glaucoma, but the disease is difficult to manage due to the inability to accurately measure IOP.²⁶ Management of chronic vision-threatening complications like glaucoma in Kpro patients is becoming increasingly important as early complications such as endophthalmitis or device extrusion are becoming less common.^{27,28} Many Kpro patients receive vitrectomies at the time of Kpro implantation. These patients may benefit enormously from the accurate measurement of IOP in the vitreous chamber.

Telemetric IOP monitors have been implanted into a small cohort of Kpro patients and offers an alternative method for direct measurement of IOP in these patients.²⁹ However, 3 of 12 devices were explanted over the course of a year, and there were concerns for potential adverse events associated with the devices. Our device may offer a safe alternative in Kpro patients. Interestingly, data from the implantable IOP monitors were compared to anterior chamber manometry.³⁰ This suggests that it may be possible to measure IOP using our device in Kpro patients even without vitrectomy.

However, serial anterior segment imaging has demonstrated progressive angle closure and shallowing of the anterior chamber in KPro patients, so anterior chamber measurements may still not be viable over the long term.³¹ Implantable devices also face issues of measurement drift over the lifetime of the device.^{32,33} Implantable devices can be re-calibrated to correct for drift by performing GAT in healthy eyes, but this is not possible in KPro patients. Our device may be useful for recalibration of implantable devices as their safety profiles become more acceptable.

The use of the term "gold standard" to describe a diagnostic technique or therapeutic intervention has been criticized as inaccurate or misleading due to the rapidly evolving state of medical care.^{34,35} Nonetheless, GAT has long been referred to as the gold standard for IOP measurement.¹ However, accurate measurement of IOP by GAT is hampered by the corneal and biomechanical artifacts discussed above. Anterior chamber cannulation manometry in animal models allows for accurate IOP measurement but was previously hampered by the invasiveness of the technique.^{36,37} Now, microfabrication techniques allow clinicians to directly measure IOP through the use of implantable devices or minimally invasive procedures. Thus a true IOP is measured rather than the surrogate IOP measured by noninvasive techniques. The small size of the handpiece and needle make this a feasible clinical measurement, with safety offered by the ability to dispose of the needle and sensor after each use. We propose that these new methods could provide a true gold standard for IOP measurement in appropriately selected patients.

This study had several limitations. First, the study was performed entirely in ex vivo models, so the

potential long-term complication rates of direct measurement of IOP in the anterior and vitreous chambers are unknown. However, the safety profiles of anterior chamber paracentesis and intravitreal injections offer promise for a similarly safe procedure that could be performed in an office setting. Second, we performed vitreous chamber measurements in only 2 eyes. The difficulty of fully closing sclerotomies after vitrectomy led to unstable eyes and variable IOP measurements at higher pressures. Eyes that are allowed to heal and develop fully watertight closures after vitrectomy are not expected to face similar inaccuracies.

Finally, the device will benefit from further miniaturization. Although the current device requires a USB connection to a computer to obtain readings, future iterations adapting advancements in wireless technology will enable further miniaturization and portability. Despite these limitations, this device offers a feasible alternative for IOP measurement in patients with altered or artificial corneas.

Acknowledgments

This work was performed in part at the San Diego Nanotechnology Infrastructure (SDNI) of UCSD, a member of the National Nanotechnology Coordinated Infrastructure, which is supported by the National Science Foundation (Grant ECCS-1542148). The work presented here was generously supported by a research grant from the state of California via AB2664. Supported in part by Research to Prevent Blindness, New York, NY.

Disclosure: **T. Gopesh**, None; **A. Camp**, None; **M. Unanian**, None; **J. Friend**, None; **R.N. Weinreb**, Implantdata (C)

References

1. Kass MA. Standardizing the measurement of intraocular pressure for clinical research: guidelines from the eye care technology forum. *Ophthalmology*. 1996;103:183–185.
2. Whitacre MM, Stein R. Sources of error with use of goldmann-type tonometers. *Surv Ophthalmol*. 1993;38:1–30.
3. Francis BA, Hsieh A, Lai M-Y, et al. Effects of corneal thickness, corneal curvature, and intraocular pressure level on Goldmann applanation tonometry and dynamic contour tonometry. *Ophthalmology*. 2007;114:20–26.
4. Medeiros FA, Weinreb RN. Evaluation of the influence of corneal biomechanical properties on intraocular pressure measurements using the ocular response analyzer. *J Glaucoma*. 2006;15:364–370.
5. Risma JM, Tehrani S, Wang K, Fingert JH, Alward WLM, Kwon YH. The utility of diaton tonometer measurements in patients with ocular hypertension, glaucoma, and glaucoma tube shunts: a preliminary study for its potential use in keratoprosthesis patients. *J Glaucoma*. 2016;25:643–647.
6. Araci IE, Su B, Quake SR, Mandel Y. An implantable microfluidic device for self-monitoring of intraocular pressure. *Nature Med*. 2014;20:1074–1078.
7. Paschalis EI, Cade F, Melki S, Pasquale LR, Dohlman CH, Ciolino JB. Reliable intraocular pressure measurement using automated radio-wave telemetry. *Clin Ophthalmol*. 2014;8:177–185.
8. Williams GA. IVT injections: health policy implications. *Rev Ophthalmol*. 2014;21:62–64.
9. Xu K, Chin EK, Bennett SR, et al. Endophthalmitis after intravitreal injection of vascular endothelial growth factor inhibitors: management and visual outcomes. *Ophthalmology*. 2018;125:1279–1286.
10. Trivedi D, Denniston AKO, Murray PI. Safety profile of anterior chamber paracentesis performed at the slit lamp. *Clin Exp Ophthalmol*. 2011;39:725–728.
11. Bui BV, Edmunds B, Cioffi GA, Fortune B. The gradient of retinal functional changes during acute intraocular pressure elevation. *Invest Ophthalmol Visual Sci*. 2005;46:202–213.
12. Tsai TI, Bui BV, Vingrys AJ. Effect of acute intraocular pressure challenge on rat retinal and cortical function. *Invest Ophthalmol Vis Sci*. 2014;55:1067–1077.
13. Crowston JG, Yu X, Kong G, et al. An acute intraocular pressure challenge to assess retinal ganglion cell injury and recovery in the mouse. *Exp Eye Res*. 2015;141:3–8.
14. Morrison JC, Cepurna WO, Tehrani S, et al. A period of controlled elevation of iop (cei) produces the specific gene expression responses and focal injury pattern of experimental rat glaucoma. *Invest Ophthalmol Vis Sci*. 2016;57:6700–6711.
15. Last JA, Liliensiek SJ, Nealey PF, Murphy CJ. Determining the mechanical properties of human corneal basement membranes with atomic force microscopy. *J Struct Biol*. 2009;167:19–24.

16. Sheng Lim K, Wickremasinghe SS, Cordeiro MF, Bunce C, Khaw PT. Accuracy of intraocular pressure measurements in new zealand white rabbits. *Invest Ophthalmol Vis Sci.* 2005;46:2419–2423.
17. Löbler M, Rehmer A, Guthoff R, Martin H, Sternberg K, Stachs O. Suitability and calibration of a rebound tonometer to measure iop in rabbit and pig eyes. *Vet Ophthalmol.* 2011;14:66–68.
18. Gunvant P, Newcomb RD, Kirstein EM, Malinovsky VE, Madonna RJ, Meetz RE. Measuring accurate IOPs: Does correction factor help or hurt? *Clin Ophthalmol.* 2010;4:611–616.
19. Gunvant P, O’leary DJ, Baskaran M, Broadway DC, Watkins RJ, Vijaya L. Evaluation of tonometric correction factors. *J Glaucoma.* 2005;14:337–343.
20. Orssengo GJ, Pye DC. Determination of the true intraocular pressure and modulus of elasticity of the human cornea in vivo. *Bull Math Biol.* 1999;61:551–572.
21. Chang DH, Stulting RD. Change in intraocular pressure measurements after lasik: the effect of the refractive correction and the lamellar flap. *Ophthalmology.* 2005;112:1009–1016.
22. Hardin JS, Lee CI, Lane LF, Hester CC, Grant MR. Corneal hysteresis in post-radial keratotomy primary open-angle glaucoma. *Graefes Arc Clin Exp Ophthalmol.* 2018;256:1971–1976.
23. Shih P-J, Wang I-J, Cai W-F, Yen J-Y. Biomechanical simulation of stress concentration and intraocular pressure in corneas subjected to myopic refractive surgical procedures. *Sci Rep.* 2017;7:13906.
24. Jain AK, Saini JS, Gupta R, et al. Tonometry in normal and scarred corneas, and in postkeratoplasty eyes: A comparative study of the Goldmann, the proton and the Schiottz tonometers. *Ind J Ophthalmol.* 2000;48:25–32.
25. Hern’andez-Verdejo JL, Teus MA, Bolivar G. Simultaneous measurement of intraocular pressure in the anterior chamber and the vitreous cavity. *Acta Ophthalmol.* 2010;88:e265–e268.
26. Netland PA, Terada H, Dohlman CH. Glaucoma associated with keratoprosthesis1. *Ophthalmology.* 1998;105:751–757.
27. Lee R, Khoueir Z, Tsikata E, Chodosh J, Dohlman CH, Chen TC. Long-term visual outcomes and complications of boston keratoprosthesis type ii implantation. *Ophthalmology.* 2017;124:27–35.
28. Gibbons A, Leung EH, Haddock LJ, et al. Long-term outcomes of the aphakic snap-on boston type i keratoprosthesis at the bascom palmer eye institute. *Clin Ophthalmol.* 2018;12:331–337.
29. Enders P, Hall J, Bornhauser M, et al. Telemetric intraocular pressure monitoring after boston keratoprosthesis surgery. *Ophthalmology.* 2019;126:322–324.
30. Lee JO, Park H, Du J, et al. A microscale optical implant for continuous in vivo monitoring of intraocular pressure. *Microsyst Nanoeng.* 2017;3:17057.
31. Kang JJ, Allemann N, Cruz JDL, Cortina MS. Serial analysis of anterior chamber depth and angle status using anterior segment optical coherence tomography after Boston keratoprosthesis. *Cornea.* 2013;32:1369–1374.
32. Crawford Downs J, Burgoyne CF, Seigfreid WP, Reynaud JF, Strouthidis NG, Sallee V. 24-hour IOP telemetry in the nonhuman primate: implant system performance and initial characterization of IOP at multiple timescales. *Invest Ophthalmol Vis Sci.* 2011;52:7365–7375.
33. Yu L, Kim B, Meng E. Chronically implanted pressure sensors: challenges and state of the field. *Sensors.* 2014;14:20620–20644.
34. Duggan PF. Time to abolish “gold standard”. *BMJ.* 1992;304:1568.
35. Jones DS, Podolsky SH. The history and fate of the gold standard. *Lancet.* 2015;385:1502–1503.
36. Peterson JA, Kiland JA, Croft MA, Kaufman PL. Intraocular pressure measurement in cynomolgus monkeys. tonopen versus manometry. *Investig Ophthalmol Vis Sci.* 37:1197–1199, 1996.
37. Morris CA, Crowston JG, Lindsey JD, Danias J, Weinreb RN. Comparison of invasive and non-invasive tonometry in the mouse. *Exp Eye Res.* 2006;82:1094–1099.